

Dark Matter Minihalos from Primordial Magnetic Fields

Pranjal Ralegankar*

SISSA, International School for Advanced Studies, via Bonomea 265, 34136 Trieste, Italy

Primordial magnetic fields (PMF) can enhance baryon perturbations on scales below the photon mean free path. However, a magnetically driven baryon fluid becomes turbulent near recombination, thereby damping out baryon perturbations below the turbulence scale. In this Letter, we show that the initial growth in baryon perturbations gravitationally induces growth in the dark matter perturbations, which are unaffected by turbulence and eventually collapse to form $10^{-11} - 10^3 M_\odot$ dark matter minihalos. If the magnetic fields purportedly detected in the blazar observations are PMFs generated after inflation and have a Batchelor spectrum, then such PMFs could potentially produce dark matter minihalos.

Introduction. Magnetic fields are found to be ubiquitous in our observations of the Universe. An intriguing possibility is that the observed cosmic magnetic fields are seeded by magnetic fields produced in the early Universe, either during inflation or phase transition [1, 2]. So far no direct evidence for the primordial nature of the magnetic fields has been obtained. However, the absence of GeV gamma-ray halos around TeV blazars might be evidence for primordial magnetic fields [3–7].

If magnetic fields have a primordial origin, then they tend to enhance baryon density perturbations after baryons decouple from photons in the early Universe [8–12]. This is because a stochastically distributed magnetic field has a compressible component of the Lorentz force acting on the baryon fluid. When baryons are strongly coupled with the photon bath, the relativistic photon pressure counteracts any growth in baryon density perturbations. But on scales below the photon mean free path, the baryon fluid is decoupled from the photon bath and the compressible Lorentz force can lead to the growth of baryon inhomogeneities.

Earlier works that studied the impact of primordial magnetic fields (PMFs) on the matter power spectrum focussed on length scales larger than the so called magnetic Jeans length and thereby focussed on structures bigger than $\sim 10^6 M_\odot$ [8, 9, 11, 13–24]. On scales smaller than the magnetic Jeans length, baryon perturbations tend to become non-linear prior to recombination [12]. However, the non-linearities in the baryon fluid eventually lead to turbulence at recombination and all signs of enhanced baryon density perturbations below the magnetic Jeans length are now erased [25, 26].

In this Letter, we show that even though the small-scale baryon density perturbations are erased, their growth history prior to recombination enhances the amplitude of dark matter (DM) density perturbations, solely through gravitational interactions. Thus, searches for DM minihalos with masses smaller than $10^6 M_\odot$ can be used to probe PMFs.

Magnetic fields in the photon drag regime. We shall focus on scales smaller than the photon mean free path and on times before recombination. Moreover, we

consider scales larger than 0.01 pc, where the baryon fluid can be approximated as a perfect fluid and a perfect conductor prior to recombination. Consequently, the motion of the baryon fluid under the influence of a PMF is given by [10]

$$\frac{\partial \vec{v}_b}{\partial t} + (H + \alpha) \vec{v}_b + \frac{c_b^2}{a} \nabla \delta_b = \frac{\vec{L}_B}{a} - \frac{\nabla \phi}{a}, \quad (1)$$

where a is the scale factor, t is the cosmic time, $\vec{v}_b = a d\vec{x}_b/dt$ is the physical baryon velocity, $\delta = (\rho(x) - \bar{\rho})/\bar{\rho}$ is the fluid density perturbation, ϕ is the metric perturbation following the convention in [27], $\alpha = 4\rho_\gamma/(3\rho_b l_\gamma)$ parametrizes the photon drag force with l_γ being the photon mean free path, ρ_γ is the photon energy density, c_b^2 is the baryon sound speed and parametrizes the baryon thermal pressure, H is the Hubble rate, and $\vec{L}_B = (\nabla \times \vec{B}) \times \vec{B}/[4\pi a^4 \rho_b]$ is the Lorentz force with $\vec{B} = a^2 \vec{B}_{\text{phys}}$ being the comoving magnetic field and \vec{B}_{phys} being the physical magnetic field. The evolution of B is determined by,

$$\frac{\partial \vec{B}}{\partial t} = \frac{1}{a} \nabla \times (\vec{v}_b \times \vec{B}). \quad (2)$$

We work in natural units where $\hbar = c = 1$.

In eq. (1) we have ignored the contribution from convection, $(\vec{v}_b \cdot \nabla) \vec{v}_b/a$, because the viscous drag on baryons due to scattering with photons, αv_b , is much larger than the convective term, or equivalently, the Reynolds number is much smaller than one [28]. One can verify this by using the fact that α is orders of magnitude larger than H prior to recombination, $\alpha/H \sim 350(a_{\text{rec}}/a)^2$.

In this section, we are interested in computing the evolution of the PMF power spectrum, $P_B(k, t)$. For simplicity, we shall focus on nonhelical PMFs, which have

$$\langle B_i(k) B_j^*(k') \rangle = \delta^3(k - k') \left(\delta_{ij} - \frac{k_i k_j}{k^2} \right) \frac{P_B(k)}{2}, \quad (3)$$

where $B_i(k) = \int d^3x B_i(x) e^{ikx}$ and $\delta^3 = (2\pi)^3 \delta^3$. With the above convention, PMF energy density is simply $\rho_B \equiv \langle B^2 \rangle / [8\pi] = \int d\Pi_q P_B(q) / [8\pi]$, where $d\Pi_q = d^3q / (2\pi)^3$.

Taking the time derivative of eq. (3) and replacing $\partial B/\partial t$ using eq. (2) would yield the evolution equations for P_B . We can make further analytical progress by noting that in eq. (1), $(\alpha + H)v_b \gg \partial v_b/\partial t \sim H v_b$ before recombination. Then if the Lorentz force dominates over thermal pressure and gravity, we have $a\vec{v}_b \approx \vec{L}_B/(\alpha + H)$. Working in this large Lorentz force limit and neglecting non-Gaussianities in the distribution of B (i.e. quasi-normal approximation), we obtain

$$\frac{\partial P_B(k)}{\partial t} = \frac{-4k^2 P_B(k)}{3(\alpha + H)} \frac{\langle B^2 \rangle}{4\pi\rho_b}. \quad (4)$$

Similar equation has been derived earlier for incompressible fluid in the viscous drag regime [29] (for analytical treatments in the turbulence regime see for example Refs. [30–32], and Ref. [33] for analytical treatment of n -point correlations).

The solution to eq. (4) is given by

$$P_B[k, k_D(t)] = P_B(k, t_i) e^{-k^2/k_D^2}, \quad (5)$$

where k_D represents the damping scale due to photon drag, and $P_B(k, t_i)$ is the power spectra prior to the photon drag regime, i.e. when the PMF coherence length scale was larger than the photon diffusion length, $l_{\gamma D} \approx 1/4\sqrt{l_\gamma/[aH]}$.

Prior to the photon drag regime, the baryon-photon plasma exhibits high Reynolds numbers. Consequently, PMFs induce turbulence in the baryon-photon plasma on small scales, with $P_B(k, t_i) \propto k^{-11/3}$ according to Kolmogorov cascade. On large scales, the power-law dependence of $P_B(k, t_i)$ is set by the physics of magnetogenesis. In this Letter, we consider PMFs with a Batchelor spectrum on large scales, $P_B(k, t_i) \propto k^2$, which is often encountered in magnetogenesis from phase transitions [1, 2, 34]. We adopt the exact shape of $P_B(k, t_i)$ from Ref. [35], and we rescale it to achieve the desired initial PMF strength, $B_I \equiv \langle B^2(t_i) \rangle$, and the initial coherence length scale, $\xi_I \equiv B_I^{-2} \int d\Pi_q P_B(q, t_i)/q$.

In magnetogenesis from phase-transitions, ξ_I is directly determined by B_I . In particular, if Alfvénic physics governs magneto-hydrodynamic (MHD) turbulence, then $\xi_I \sim V_{AI}/[aH]_i$, with $V_{AI} = B_I/\sqrt{4\pi a^4(\rho_b + 4\rho_\gamma/3)}$ [28, 36]. Recently, it has been argued that a reconnection-controlled MHD turbulence leads to a better agreement with simulations [37, 38], leading to $\xi_I \sim 0.1V_{AI}/[aH]_i$ for B_I values of our interest [39]. Due to uncertainties in turbulence theory, we keep ξ_I as a free parameter. This also allows us to consider inflationary magnetogenesis scenarios, which can produce $\xi_I \gg V_{AI}/[aH]_i$.

In the photon drag regime, the damping scale can become the new coherence scale if k_D^{-1} exceeds ξ_I . Substituting eq. (5) back in eq. (4), we obtain

$$a \frac{\partial}{\partial a} \left(\frac{1}{k_D^2} \right) = \frac{4V_A^2/3}{a^2 H(\alpha + H)}, \quad (6)$$

where $V_A^2 = \langle B^2 \rangle/(4\pi a^4 \rho_b)$ is the Alfvén speed. Given that $a\vec{v}_b \approx \vec{L}_B/(\alpha + H)$ and $L_B \sim k_D V_A^2$, eq. (6) tells us that the damping scale is roughly the distance a baryon particle travels in a Hubble time, $ak_D^{-1} \sim v_b/H \sim k_D V_A^2/[aH(\alpha + H)]$. The above equation agrees with the free-streaming Alfvén damping scale derived for pre-recombination universe ($\alpha \gg H$) by Ref. [40], as well as with the magnetic Jeans damping scale derived for post-recombination universe ($\alpha \ll H$) by Ref. [9, 10].

We have neglected the effect of thermal pressure and gravity while deriving eq. (6). We find that even if thermal pressure dominates over the Lorentz force, the damping scale remains largely unchanged [41] (see also [29, 40]). Furthermore, for PMFs that produce observable enhancement in the DM power spectrum, we find gravity to overcome the Lorentz force only after $k \gg k_D$. Consequently, we approximate the damping scale to be given by eq. (6) in all regimes.

In the top panel of figure 1, the green line shows the evolution of the damping scale, k_D^{-1} . We have solved the background cosmology parameters (H , α , ρ , etc.) using CLASS [42]. One can see that k_D^{-1} grows as $a^{3/2}$ when $k_D^{-1} \lesssim \xi_I$ and as $k_D^{-1} \propto a^{3/7}$ after $k_D^{-1} > \xi_I$. This transition occurs because when $k_D^{-1} < \xi_I$ the PMF is flux frozen (constant $\langle B^2 \rangle$) but afterwards the PMF is damped as $\langle B^2 \rangle \propto k_D^5 \propto a^{-15/14}$. The sudden increase in k_D^{-1} near recombination is due to the rapid decrease in photon drag, α .

After recombination, the rapid decrease in α causes the Reynolds number of the plasma to become larger than one [28]. Thus, the MHD fluid becomes turbulent and this turbulence is not captured in our formalism. Nevertheless, we extend eq. (6) beyond recombination and find a logarithmic growth of k_D^{-1} , which is also expected from simulations [28]. Consequently, our evaluation of present-day values of B and k_D should be accurate up to an order of magnitude.

Impact on baryon density perturbations. The continuity equation for δ_b in the linear limit is

$$\frac{\partial \delta_b}{\partial t} + \frac{\nabla \cdot \vec{v}_b}{a} = 0. \quad (7)$$

We find that the nonlinear term in the continuity equation, $\nabla \cdot (\delta_b \vec{v}_b)/a$, tends to enhance the power spectrum of δ_b by $\sim 10\%$ when baryons are driven by the Lorentz force [41]. We found this by taking the ensemble average of the continuity equation convolved with $\delta_b(x')$ and using the linear solution, $\delta_b \propto \nabla \cdot v_b/[aH] = a^{-2} \nabla \cdot L_B/[H(\alpha + H)]$. As we are not interested in a precision calculation of the DM power spectrum, we have ignored the nonlinear term here.

In the bottom panel of figure 1, we show the evolution of $\hat{\delta}_b \equiv \sqrt{k^3 P_b(k)/(2\pi^2)}$ for two different Fourier modes, where P_b is the baryon power spectrum. We start our computation when the photon mean free path exceeds the initial coherence length scale, $l_\gamma(t'_i) > \xi_I$. We set $\delta_b(t'_i) =$

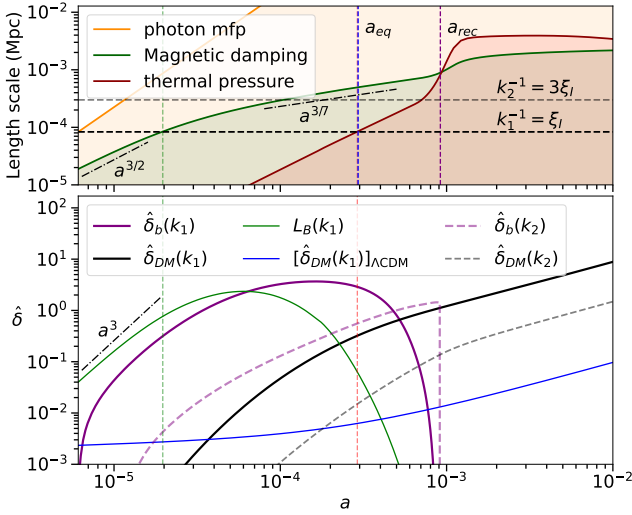


FIG. 1. Here, $B_I = 5$ nG and $\xi_I = 10^{-4}$ Mpc. **Top:** Evolution of the photon mean free path (orange), the magnetic damping scale k_D^{-1} (green), and the thermal pressure damping scale λ_{th} (red). Horizontal dashed lines mark the comoving wave numbers corresponding to perturbations shown in the bottom panel. **Bottom:** Evolution of the square root of dimensionless power spectra, $\hat{\delta} = \sqrt{k^3 P / (2\pi^2)}$. The green line shows $\hat{\delta}$ for $a^{-2} \nabla \cdot \vec{L}_B / [H(\alpha + H)]$. The blue line shows $\hat{\delta}_{DM}$ in a universe with no PMF, while other lines correspond to perturbations sourced by PMFs assuming trivial initial condition. Vertical green and red dashed lines mark the time when k_1^{-1} crosses k_D^{-1} and λ_{th} , respectively.

$v_b(t'_i) = 0$, which is expected due to silk damping. Here v_b is solved using eq. (1).

The evolution of δ_b can roughly be classified into four regimes. In the first regime, δ_b grows as $\sim a^3$ due to the Lorentz force. Growth stops when the damping scale exceeds the length scale of the Fourier mode, $k_D^{-1} \gtrsim 3k^{-1}$, as the Lorentz force is damped out.

Our evaluation of $\hat{\delta}_b$ for $k_D^{-1} \gtrsim k$ is not completely accurate. This is because we have approximated the evolution of $L_B(k, t)$ to be the same as $\sqrt{\langle L_B^2(k, t) \rangle}$, which is not true due to nonlinear processing between different Fourier modes of PMF. However, this approximation is acceptable for calculating $P_b(k, t)$, as $\delta_b \propto a^{-2} \nabla \cdot \vec{L}_B / (\alpha + H)$ when baryons are driven by L_B . Consequently, P_b is directly determined by $\langle L_B^2(k, t) \rangle$. Furthermore, once L_B is damped for $k \gg k_D$, δ_b becomes insensitive to our approximation in $L_B(k)$. In the transition regime, we expect no more than $\mathcal{O}(1)$ correction to P_b .

The second regime of δ_b evolution corresponds to saturation, where v_b is quickly driven to zero by the photon drag and δ_b saturates to a constant. If baryon thermal pressure is ignored, δ_b asymptotes to $\sim \mathcal{O}(1)$ values for $k \gg k_D$. The $\mathcal{O}(1)$ asymptote reflects the fact that k_D is determined by the distance traveled by a baryon particle

in a Hubble time, $k_D^{-1} \sim v_b / (aH)$, which translates to $\delta_b \sim \mathcal{O}(1)$ as $\delta_b \sim kv_b / (aH)$.

The third regime corresponds to the damping of δ_b by thermal pressure. The thermal pressure becomes important when it is comparable to the photon drag force, $c_b^2 k \delta_b \sim (H + \alpha)v_b$. Using $\delta_b \sim kv_b / (aH)$, we find the thermal pressure damping scale to be

$$\lambda_{th} = \frac{c_b}{aH} \sqrt{\frac{H}{\alpha + H}}. \quad (8)$$

We plot this scale as a red line in the top panel of figure 1.

Finally, the fourth regime corresponds to turbulence damping near recombination. At recombination, the photon drag force almost instantaneously becomes negligible and the convective terms in the baryon Euler equation (eq. (1)) can no longer be ignored [25, 26, 28]. We model the impact of turbulence on δ_b by setting $\delta_b = 0$ at recombination for all scales inside the magnetic damping scale.

Impact on DM perturbations. The rapid growth in δ_b gravitationally induces growth in DM perturbations, δ_{DM} . We find that δ_{DM} largely remains in the perturbative regime before recombination even if δ_b reaches non-linear values. This is because the gravitational influence of baryons is suppressed by a factor of ρ_b / ρ_{tot} . Consequently, the growth in δ_{DM} is well captured by the linear theory [43, 44],

$$\begin{aligned} \frac{\partial^2 \delta_{DM}}{\partial y^2} + \frac{2 + 3y}{2y(y + 1)} \frac{\partial \delta_{DM}}{\partial y} - \frac{3}{2y(y + 1)} \frac{\Omega_{DM}}{\Omega_m} \delta_{DM} \\ = \frac{3}{2y(y + 1)} \frac{\Omega_b}{\Omega_m} \delta_b. \end{aligned} \quad (9)$$

Here Ω corresponds to the present-day fraction of species, with $\Omega_b h^2 = 0.022$, $\Omega_{DM} h^2 = 0.12$, $\Omega_m = \Omega_b + \Omega_{DM}$, and $y = a/a_{eq}$ with a_{eq} being the scale factor at matter radiation equality [45].

Since δ_{DM} follows an ordinary differential equation, its solution can simply be written as a linear combination of the homogenous solution provided by the initial condition and the inhomogeneous solution indirectly sourced by PMF, $\delta_{DM} = (\delta_{DM})_{\Lambda CDM} + (\delta_{DM})_B$. As the PMF distribution is uncorrelated with the curvature perturbations determining initial conditions [45], the two solutions of δ_{DM} are uncorrelated as well [46].

In figure 2, we show the DM transfer function, $T^2(k) = P_{DM}(k) / [P_{DM}(k)]_{\Lambda CDM}$, where P_{DM} is the DM power spectrum, $\delta^3(k - k') P_{DM}(k) = \langle \delta_{DM}(k) \delta_{DM}(k') \rangle_B + \langle \delta_{DM}(k) \delta_{DM}(k') \rangle_{\Lambda CDM}$. The transfer function is quite narrowly peaked with the peak typically occurring at $k_{pk} \sim \xi_I^{-1}$. For $k < k_{pk}$, thermal pressure or turbulence at recombination suppresses δ_b before it attains its maximum value due to the Lorentz force. The value of k_{pk} for the black dashed line is shifted to $k_{pk} > \xi_I^{-1}$, because $\delta_b(k = \xi_I^{-1})$ is prematurely suppressed by tur-

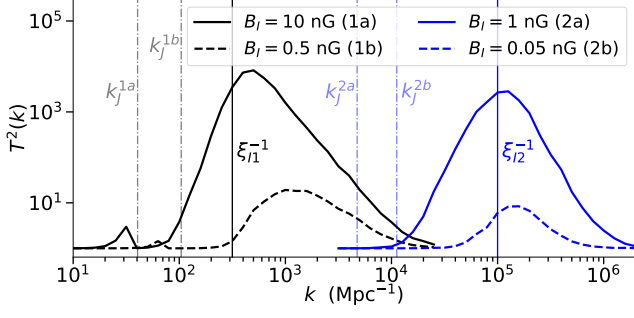


FIG. 2. The dark matter transfer function for PMF configurations sampling the edges of the parameter space shown in figure 3. The dot-dashed lines mark the magnetic Jeans scale, $\sim k_J = k_D(2a_{\text{rec}})$.

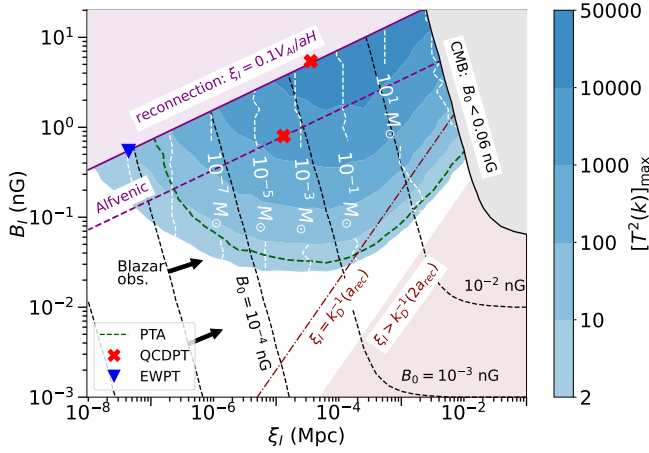


FIG. 3. Colored contours of the maximum value of dark matter transfer function as a function of initial comoving magnetic field strength, B_I , and initial coherence length scale, ξ_I . Here initial refers to the time before recombination, when the photon diffusion length exceeds ξ_I . White contours show the mass scales at which the transfer function reaches its peak. Black dashed lines show the contours of present-day magnetic field strength, B_0 . The region inside the green-dashed line produces dark matter minihalos potentially within the observable reach of PTAs. Solid and dashed purple lines denote the relation between ξ_I and B_I depending on whether MHD turbulence is determined by reconnection or Alfvénic physics, respectively. The red crosses (blue triangle) mark the maximum values of B_I for PMFs produced during QCD (electroweak) phase transition.

bulence at recombination. The value of $T(k)$ for $k > \xi_I$ is suppressed because the initial PMF is itself suppressed.

Connecting PMFs with DM minihalos. In figure 3 we vary over different initial PMF configurations and plot the contours showing the maximum enhancement to the DM transfer function, $[T^2(k)]_{\text{max}}$. A large value of $[T^2(k)]_{\text{max}}$ implies that the halos corresponding to the peak scale, k_{pk}^{-1} , collapse earlier than in the standard cos-

mology and consequently have much larger central densities [47–49]. The mass of these first formed minihalos is approximately given by the DM mass enclosed in a radius of ak_{pk}^{-1} , i.e. $M_h = 4\pi\rho_{\text{DM}}(a=1)k_{\text{pk}}^{-3}/3$.

The value of $[T^2(k)]_{\text{max}}$ is suppressed for small B_I and for both large and small ξ_I . When $B_I < 0.05$ nG, the thermal pressure inhibits the growth in $\delta_b(k_{\text{pk}})$ before it attains its $\mathcal{O}(1)$ saturation value, which then limits the growth in δ_{DM} . For $\xi_I < 10^{-4}$ Mpc, $\delta_b(k_{\text{pk}})$ is suppressed by thermal pressure before a_{eq} . Consequently, the gravitational influence of baryons on DM is suppressed by a factor of $\sim a/a_{\text{eq}}$. Finally, for $\xi_I \gtrsim k_D^{-1}(a_{\text{rec}})$, turbulence near recombination suppresses δ_b before it can attain $\mathcal{O}(1)$ values. Thus, we have restricted our analysis to $\xi_I < k_D^{-1}(2a_{\text{rec}})$.

Additionally, ξ_I has a natural lower bound for a given value of B_I . In particular, prior to the photon drag regime, PMFs induce turbulent motion in the plasma and are damped by Kolmogorov cascade below the turbulence scale. Thus, ξ_I has to be larger than the purple lines in figure 3, depending on the physics controlling MHD turbulence.

If PMFs are generated after inflation, then turbulence typically determines the coherence length scale of PMFs and B_I and ξ_I would lie on one of the purple lines. For instance, considering magnetogenesis at QCD phase transition, the largest value of B is obtained by assuming $\rho_B = \rho_{\text{SM}}$ and $\xi = (aH)^{-1}$ at $T_{\text{QCD}} = 150$ MeV. The subsequent turbulent evolution increases ξ while conserving $B^4\xi^5$ ($B^2\xi^5$) for reconnection-controlled (Alfvénic) turbulence [37].

PMFs generated after inflation can explain the absence of GeV gamma-ray halos around TeV blazars, if their present day strength, $B_0 = \langle B^2(a=1) \rangle$, is larger than $\sim 10^{-5}$ nG [50]. One can see from figure 3 that PMFs generated after electroweak phase transition (EWPT) can explain Blazar observations [39] and also enhance $T^2(k)$.

An enhancement in $T^2(k)$ implies an enhanced abundance of minihalos today. The presence of such minihalos in the Milkyway can potentially be observed by astrometric microlensing searches [51–53], caustic microlensing [54, 55], or by pulsar timing arrays (PTAs) [56–59]. For instance, the region inside the green-dashed line has $P_{\text{DM}}(k)$ which is potentially in the observable window of future PTA measurements [59]. Note that this is an optimistic estimate [60], and a more detailed analysis is required to draw any definitive conclusion on observability.

The current strongest constraint restricts $B_0 < 0.06$ nG at 95% confidence level for PMFs with a Batchelor spectrum [61]. Further stringent constraint of $B_0 < 0.01$ nG can be applied if we take into account that non-linear values of δ_b can alter recombination [25]. Recently, this fact has instead been utilized to help resolve the Hubble tension [62]. Depending on the exact values of B_I and

ξ_I that resolve the Hubble tension, it is possible that an observable abundance of DM minihalos is also produced.

Discussion. We have shown for the first time that primordial magnetic fields (PMFs) can enhance the present-day matter power spectrum on scales below the magnetic Jeans length. This implies a larger abundance of DM minihalos today.

The abundance of DM minihalos is determined not by the present-day strength of the PMF, but rather by its strength in the early Universe when baryon perturbations on the PMF coherence scale decoupled from photons. As PMFs had underwent less dissipation at that time, they had a larger potential to overcome baryon thermal pressure and generate baryon inhomogeneities. DM acts as a “memory foam” and preserves the growth history of these inhomogeneities. As a result, DM minihalos can probe PMFs with present-day strengths much below those probed by cosmic microwave background (CMB) and Faraday rotation.

Considering nonhelical PMFs that are generated after inflation with a Batchelor spectrum, we estimate that PMFs that can explain blazar observations should also produce DM minihalos heavier than $10^{-10} M_\odot$. These minihalos may be detectable through future PTA measurements.

Our results are based on analytical calculations, with the primary assumption that the distribution of PMFs remains Gaussian. Our analytical approach agrees with previous results in the literature, suggesting that non-Gaussian effects have a limited role in the photon drag regime. Consequently, even with dedicated MHD simulations, we anticipate that the qualitative relationship between the DM power spectrum and present-day PMF strengths will remain largely unchanged. However, there may be some variation in the quantitative relationship, possibly within an order of magnitude.

Even if non-gaussianities in the PMF distribution are significant, we expect the DM minihalos to still be produced below the magnetic jeans scale. This is simply because the magnetic jeans scale is set by the scale where baryon perturbations become large enough to backreact onto the magnetic fields. These large baryon perturbations gravitationally enhance DM perturbations. Subsequently, even after baryon perturbations are damped by PMFs, the gravitational potential from DM is sufficient to sustain the growth in DM perturbations and cause their eventual collapse into minihalos.

Thus, a future detection of DM minihalos should serve as a smoking gun signal for a primordial origin of cosmic magnetic fields. It is rather ironic how we can utilize the invisible component of our Universe to search for a component of the visible sector.

Acknowledgments The author thanks Karsten Jedamzik for clarification about initial magnetic field configurations and cross-checking some calculations, Kandaswamy

Subramanian for initial guidance on relevant literature, Takeshi Kobayashi for several helpful discussions, Adrienne Erickcek for clarification on minihalos and helpful discussions, Andrea Mitridate for clarification about PTA sensitivities, and Andrey Saveliev for clarifications about his work and highlighting different conventions used for PMF power spectra. The author is also thankful to Karsten Jedamzik, Takeshi Kobayashi, and Jan Schutte-Engel for helpful feedback on the manuscript.

* pralegan@sissa.it

- [1] T. Vachaspati, Progress on cosmological magnetic fields, Rept. Prog. Phys. **84**, 074901 (2021), arXiv:2010.10525 [astro-ph.CO].
- [2] K. Subramanian, The origin, evolution and signatures of primordial magnetic fields, Rept. Prog. Phys. **79**, 076901 (2016), arXiv:1504.02311 [astro-ph.CO].
- [3] A. Neronov and I. Vovk, Evidence for strong extragalactic magnetic fields from fermi observations of tev blazars, Science **328**, 73 (2010), <https://www.science.org/doi/pdf/10.1126/science.1184192>.
- [4] A. Abramowski *et al.* (H.E.S.S.), Search for Extended γ -ray Emission around AGN with H.E.S.S. and Fermi-LAT, Astron. Astrophys. **562**, A145 (2014), arXiv:1401.2915 [astro-ph.HE].
- [5] J. D. Finke, L. C. Reyes, M. Georganopoulos, K. Reynolds, M. Ajello, S. J. Fegan, and K. McCann, Constraints on the Intergalactic Magnetic Field with Gamma-Ray Observations of Blazars, Astrophys. J. **814**, 20 (2015), arXiv:1510.02485 [astro-ph.HE].
- [6] S. Archambault *et al.* (VERITAS), Search for Magnetically Broadened Cascade Emission From Blazars with VERITAS, Astrophys. J. **835**, 288 (2017), arXiv:1701.00372 [astro-ph.HE].
- [7] R. Alves Batista and A. Saveliev, The Gamma-ray Window to Intergalactic Magnetism, Universe **7**, 223 (2021), arXiv:2105.12020 [astro-ph.HE].
- [8] I. Wasserman, On the origins of galaxies, galactic angular momenta, and galactic magnetic fields., Astrophys. J. **224**, 337 (1978).
- [9] E.-j. Kim, A. Olinto, and R. Rosner, Generation of density perturbations by primordial magnetic fields, Astrophys. J. **468**, 28 (1996), arXiv:astro-ph/9412070.
- [10] K. Subramanian and J. D. Barrow, Magnetohydrodynamics in the early universe and the damping of non-linear Alfvén waves, Phys. Rev. D **58**, 083502 (1998), arXiv:astro-ph/9712083.
- [11] R. Gopal and S. K. Sethi, Large Scale Magnetic Fields: Density Power Spectrum in Redshift Space, Journal of Astrophysics and Astronomy **24**, 51 (2003).
- [12] K. Jedamzik and T. Abel, Small-scale primordial magnetic fields and anisotropies in the cosmic microwave background radiation, **2013**, 050 (2013).
- [13] S. K. Sethi and K. Subramanian, Primordial magnetic fields in the post-recombination era and early reionization, Mon. Not. Roy. Astron. Soc. **356**, 778 (2005), arXiv:astro-ph/0405413.
- [14] H. Tashiro and N. Sugiyama, Early reionization with primordial magnetic fields, Mon. Not. Roy. Astron. Soc.

- 368**, 965 (2006), arXiv:astro-ph/0512626 [astro-ph].
- [15] D. R. G. Schleicher, R. Banerjee, and R. S. Klessen, Influence of primordial magnetic fields on 21 cm emission, *Astrophys. J.* **692**, 236 (2009), arXiv:0808.1461 [astro-ph].
 - [16] S. K. Sethi and K. Subramanian, Primordial magnetic fields and the HI signal from the epoch of reionization, *JCAP* **2009** (11), 021, arXiv:0911.0244 [astro-ph.CO].
 - [17] J. R. Shaw and A. Lewis, Constraining Primordial Magnetism, *Phys. Rev. D* **86**, 043510 (2012), arXiv:1006.4242 [astro-ph.CO].
 - [18] K. L. Pandey and S. K. Sethi, Theoretical Estimates of Two-point Shear Correlation Functions using Tangled Magnetic Fields, *Astrophys. J.* **748**, 27 (2012), arXiv:1201.3619 [astro-ph.CO].
 - [19] K. L. Pandey and S. K. Sethi, Probing Primordial Magnetic Fields Using Ly α Clouds, *Astrophys. J.* **762**, 15 (2013), arXiv:1210.3298 [astro-ph.CO].
 - [20] S. Chongchitnan and A. Meiksin, The effect of cosmic magnetic fields on the metagalactic ionization background inferred from the Lyman α forest, *Mon. Not. Roy. Astron. Soc.* **437**, 3639 (2014), arXiv:1311.1504 [astro-ph.CO].
 - [21] K. L. Pandey, T. R. Choudhury, S. K. Sethi, and A. Ferrara, Reionization constraints on primordial magnetic fields, *Mon. Not. Roy. Astron. Soc.* **451**, 1692 (2015), arXiv:1410.0368 [astro-ph.CO].
 - [22] T. Minoda, K. Hasegawa, H. Tashiro, K. Ichiki, and N. Sugiyama, Thermal Sunyaev-Zel'dovich effect in the intergalactic medium with primordial magnetic fields, *Phys. Rev. D* **96**, 123525 (2017), arXiv:1705.10054 [astro-ph.CO].
 - [23] M. Sanati, Y. Revaz, J. Schober, K. E. Kunze, and P. Jablonka, Constraining the primordial magnetic field with dwarf galaxy simulations, *Astronomy and Astrophysics* **643**, A54 (2020).
 - [24] H. Katz, S. Martin-Alvarez, J. Rosdahl, T. Kimm, J. Blaizot, M. G. Haehnelt, L. Michel-Dansac, T. Garel, J. Oñorbe, J. Devriendt, A. Slyz, O. Attia, and R. Teyssier, Introducing SPHINX-MHD: the impact of primordial magnetic fields on the first galaxies, reionization, and the global 21-cm signal, *Mon. Not. Roy. Astron. Soc.* **507**, 1254 (2021), arXiv:2101.11624 [astro-ph.CO].
 - [25] K. Jedamzik and A. Saveliev, Stringent Limit on Primordial Magnetic Fields from the Cosmic Microwave Background Radiation, *Phys. Rev. Lett.* **123**, 021301 (2019), arXiv:1804.06115 [astro-ph.CO].
 - [26] P. Trivedi, J. Reppin, J. Chluba, and R. Banerjee, Magnetic heating across the cosmological recombination era: Results from 3D MHD simulations, *Mon. Not. Roy. Astron. Soc.* **481**, 3401 (2018), arXiv:1805.05315 [astro-ph.CO].
 - [27] C.-P. Ma and E. Bertschinger, Cosmological perturbation theory in the synchronous and conformal Newtonian gauges, *Astrophys. J.* **455**, 7 (1995), arXiv:astro-ph/9506072.
 - [28] R. Banerjee and K. Jedamzik, The Evolution of cosmic magnetic fields: From the very early universe, to recombination, to the present, *Phys. Rev. D* **70**, 123003 (2004), arXiv:astro-ph/0410032.
 - [29] L. Campanelli, Evolution of primordial magnetic fields in mean-field approximation, *Eur. Phys. J. C* **74**, 2690 (2014), arXiv:1304.4044 [astro-ph.CO].
 - [30] L. Campanelli, Evolution of Magnetic Fields in Freely Decaying Magnetohydrodynamic Turbulence, *Phys. Rev. Lett.* **98**, 251302 (2007), arXiv:0705.2308 [astro-ph].
 - [31] K. Jedamzik and G. Sigl, The Evolution of the Large-Scale Tail of Primordial Magnetic Fields, *Phys. Rev. D* **83**, 103005 (2011), arXiv:1012.4794 [astro-ph.CO].
 - [32] A. Saveliev, K. Jedamzik, and G. Sigl, Evolution of Helical Cosmic Magnetic Fields as Predicted by Magnetohydrodynamic Closure Theory, *Phys. Rev. D* **87**, 123001 (2013), arXiv:1304.3621 [astro-ph.CO].
 - [33] P. Berger, A. Kehagias, and A. Riotto, Testing the Origin of Cosmological Magnetic Fields through the Large-Scale Structure Consistency Relations, *JCAP* **05**, 025, arXiv:1402.1044 [astro-ph.CO].
 - [34] R. Durrer and C. Caprini, Primordial magnetic fields and causality, *JCAP* **11**, 010, arXiv:astro-ph/0305059.
 - [35] S. Mchedlidze, P. Domínguez-Fernández, X. Du, A. Brandenburg, T. Kahniashvili, S. O'Sullivan, W. Schmidt, and M. Brüggen, Evolution of Primordial Magnetic Fields during Large-scale Structure Formation, *Astrophys. J.* **929**, 127 (2022), arXiv:2109.13520 [astro-ph.CO].
 - [36] T. Kahniashvili, A. G. Tevzadze, A. Brandenburg, and A. Neronov, Evolution of Primordial Magnetic Fields from Phase Transitions, *Phys. Rev. D* **87**, 083007 (2013), arXiv:1212.0596 [astro-ph.CO].
 - [37] D. N. Hosking and A. A. Schekochihin, Reconnection-controlled decay of magnetohydrodynamic turbulence and the role of invariants, *Phys. Rev. X* **11**, 041005 (2021).
 - [38] H. Zhou, R. Sharma, and A. Brandenburg, Scaling of the Hosking integral in decaying magnetically dominated turbulence, *J. Plasma Phys.* **88**, 905880602 (2022), arXiv:2206.07513 [physics.plasm-ph].
 - [39] D. N. Hosking and A. A. Schekochihin, Cosmic-void observations reconciled with primordial magnetogenesis, (2022), arXiv:2203.03573 [astro-ph.CO].
 - [40] K. Jedamzik, V. Katalinic, and A. V. Olinto, Damping of cosmic magnetic fields, *Phys. Rev. D* **57**, 3264 (1998), arXiv:astro-ph/9606080.
 - [41] See supplemental material for the analytically derived evolution of maximally helical magnetic fields, for the derivation of damping scale when thermal pressure is dominant, and for the estimate of the non-linear term in the baryon continuity equation., .
 - [42] D. Blas, J. Lesgourgues, and T. Tram, The Cosmic Linear Anisotropy Solving System (CLASS). Part II: Approximation schemes, *JCAP* **2011** (7), 034, arXiv:1104.2933 [astro-ph.CO].
 - [43] W. Hu and N. Sugiyama, Small scale cosmological perturbations: An Analytic approach, *Astrophys. J.* **471**, 542 (1996), arXiv:astro-ph/9510117.
 - [44] P. Meszaros, The behaviour of point masses in an expanding cosmological substratum, *Astron. Astrophys.* **37**, 225 (1974).
 - [45] N. Aghanim *et al.* (Planck), Planck 2018 results. VI. Cosmological parameters, (2018), arXiv:1807.06209 [astro-ph.CO].
 - [46] K. E. Kunze, Magnetic field back reaction on the matter power spectrum, *JCAP* **09**, 047, arXiv:2207.09859 [astro-ph.CO].
 - [47] J. S. Bullock, T. S. Kolatt, Y. Sigad, R. S. Somerville, A. V. Kravtsov, A. A. Klypin, J. R. Primack, and A. Dekel, Profiles of dark haloes. Evolution, scatter, and environment, *Mon. Not. Roy. Astron. Soc.* **321**, 559

- (2001), arXiv:astro-ph/9908159.
- [48] R. H. Wechsler, J. S. Bullock, J. R. Primack, A. V. Kravtsov, and A. Dekel, Concentrations of dark halos from their assembly histories, *Astrophys. J.* **568**, 52 (2002), arXiv:astro-ph/0108151.
- [49] M. S. Delos, M. Bruff, and A. L. Erickcek, Predicting the density profiles of the first halos, *Phys. Rev. D* **100**, 023523 (2019), arXiv:1905.05766 [astro-ph.CO].
- [50] A. M. Taylor, I. Vovk, and A. Neronov, Extragalactic magnetic fields constraints from simultaneous GeV-TeV observations of blazars, *Astron. Astrophys.* **529**, A144 (2011), arXiv:1101.0932 [astro-ph.HE].
- [51] A. L. Erickcek and N. M. Law, Astrometric Microlensing by Local Dark Matter Subhalos, *Astrophys. J.* **729**, 49 (2011), arXiv:1007.4228 [astro-ph.CO].
- [52] F. Li, A. L. Erickcek, and N. M. Law, A new probe of the small-scale primordial power spectrum: astrometric microlensing by ultracompact minihalos, *Phys. Rev. D* **86**, 043519 (2012), arXiv:1202.1284 [astro-ph.CO].
- [53] K. Van Tilburg, A.-M. Taki, and N. Weiner, Halometry from Astrometry, *JCAP* **07**, 041, arXiv:1804.01991 [astro-ph.CO].
- [54] M. Oguri, J. M. Diego, N. Kaiser, P. L. Kelly, and T. Broadhurst, Understanding caustic crossings in giant arcs: characteristic scales, event rates, and constraints on compact dark matter, *Phys. Rev. D* **97**, 023518 (2018), arXiv:1710.00148 [astro-ph.CO].
- [55] J. M. Diego *et al.*, Dark Matter under the Microscope: Constraining Compact Dark Matter with Caustic Crossing Events, *Astrophys. J.* **857**, 25 (2018), arXiv:1706.10281 [astro-ph.CO].
- [56] E. R. Siegel, M. P. Hertzberg, and J. N. Fry, Probing Dark Matter Substructure with Pulsar Timing, *Mon. Not. Roy. Astron. Soc.* **382**, 879 (2007), arXiv:astro-ph/0702546.
- [57] H. A. Clark, G. F. Lewis, and P. Scott, Investigating dark matter substructure with pulsar timing – I. Constraints on ultracompact minihaloes, *Mon. Not. Roy. Astron. Soc.* **456**, 1394 (2016), [Erratum: *Mon. Not. Roy. Astron. Soc.* **464**, 2468 (2017)], arXiv:1509.02938 [astro-ph.CO].
- [58] H. Ramani, T. Trickle, and K. M. Zurek, Observability of Dark Matter Substructure with Pulsar Timing Correlations, *JCAP* **12**, 033, arXiv:2005.03030 [astro-ph.CO].
- [59] V. S. H. Lee, A. Mitridate, T. Trickle, and K. M. Zurek, Probing Small-Scale Power Spectra with Pulsar Timing Arrays, *JHEP* **06**, 028, arXiv:2012.09857 [astro-ph.CO].
- [60] V. S. H. Lee, S. R. Taylor, T. Trickle, and K. M. Zurek, Bayesian Forecasts for Dark Matter Substructure Searches with Mock Pulsar Timing Data, *JCAP* **08**, 025, arXiv:2104.05717 [astro-ph.CO].
- [61] D. Paoletti, J. Chluba, F. Finelli, and J. A. Rubiño Martín, Constraints on Primordial Magnetic Fields from their impact on the ionization history with Planck 2018 10.1093/mnras/stac2947 (2022), arXiv:2204.06302 [astro-ph.CO].
- [62] K. Jedamzik and L. Pogosian, Relieving the Hubble tension with primordial magnetic fields, *Phys. Rev. Lett.* **125**, 181302 (2020), arXiv:2004.09487 [astro-ph.CO].
- [63] P. A. R. Ade *et al.* (Planck), Planck 2015 results. XIX. Constraints on primordial magnetic fields, *Astron. Astrophys.* **594**, A19 (2016), arXiv:1502.01594 [astro-ph.CO].

Magnetic damping scale for incompressible fluid

In this section we derive the evolution of non-helical magnetic field power spectrum for scenarios where the baryon thermal pressure dominates over the Lorentz force in the photon drag regime.

In the main Letter we showed that the baryon velocity is determined by the balance between the Lorentz force and the photon drag force, $a\vec{v}_b \approx \vec{L}_B/(\alpha + H)$, when thermal pressure is negligible. In contrast, in the strong thermal pressure limit, compressible motion in the baryons is suppressed, $\nabla \cdot v_b \rightarrow 0$. However, the Lorentz force can **still** induce divergence free motion in the baryon fluid without hindrance. Consequently, one can write the Fourier transformed baryon velocity vector as

$$v_{b,j}(q) = \left(\delta_{lj} - \frac{q_l q_j}{q^2} \right) \frac{L_{B,l}(q)}{a(\alpha + H)} = \hat{p}_{lj}(q) \frac{L_{B,l}(q)}{a(\alpha + H)}, \quad (10)$$

where $\vec{L}_B(q)$ is the Fourier transform of the Lorentz force, $\vec{L}_B(x) = (\nabla \times \vec{B}) \times \vec{B}/[4\pi a^4 \rho_b]$.

The motion in the baryon fluid feeds back onto the magnetic field via the induction equation, eq. (2). Taking the Fourier transform of eq. (2) and replacing v_b using eq. (10), we obtain

$$\frac{\partial B_i(k)}{\partial t} = \frac{-k_m}{(4\pi \rho_b)(\alpha + H)} [\delta_{ml} \delta_{ji} - \delta_{mj} \delta_{li}] [\delta_{ab} \delta_{nc} - \delta_{bc} \delta_{na}] \int d\Pi_{q_1} d\Pi_{q_2} \hat{p}_{jn}(q_1) q_{2a} B_b(q_1 - q_2) B_c(q_2) B_l(k - q_1), \quad (11)$$

where $d\Pi_q = d^3q/(2\pi)^3$.

To obtain the evolution of the power spectrum, we use the fact that

$$\delta^3(k - k') \frac{\partial P_B(k)}{\partial t} = \frac{1}{2} \left\langle \frac{\partial B_m(k)}{\partial t} B_m^*(k') \right\rangle. \quad (12)$$

Then replacing the derivative of B using eq. (11), using $\langle B_i(k) B_j^*(k') \rangle \equiv \delta^3(k - k') M_{ij}(k')$, and assuming magnetic

fields to be Gaussian distributed, we obtain

$$\begin{aligned} \frac{\partial P_B(k)}{\partial t} = & \frac{-\delta^3(k-k')}{2(4\pi\rho_b)(\alpha+H)} k_i [\delta_{il}\delta_{jm} - \delta_{ij}\delta_{lm}] [\delta_{ab}\delta_{nc} - \delta_{bc}\delta_{na}] \\ & \times \int d\Pi_q \hat{p}_{jn}(k-q) [k_a M_{lb}(q) M_{cm}(k) - q_a M_{lc}(q) M_{bm}(k)]. \end{aligned} \quad (13)$$

Next, considering non-helical fields, we replace M using eq. (3) and set $h = 0$. Doing so yields

$$\frac{\partial P_B(k)}{\partial t} = \frac{-P_B(k)}{(4\pi\rho_b)(\alpha+H)} \int d\Pi_q \left[-\frac{2}{3}(k^2 + 3q^2) + \frac{(k^4 + k^2q^2 + q^4)}{kq} \ln \left(\frac{k^2 + q^2 + kq}{k^2 + q^2 - kq} \right) \right] P_B(q). \quad (14)$$

To obtain a simple expression we can look at the asymptotic limit, $k \ll k_D$ or $k \gg k_D$. In these limits, the integral is dominated by the phase space where $q \sim k_D \gg k$ or $q \sim k_D \ll k$. Both limits yield

$$\frac{\partial P_B(k)}{\partial t} \approx -\frac{4k^2 V_A^2}{3a^2(\alpha+H)} P(k), \quad (15)$$

where $V_A^2 = \langle B^2 \rangle / [4\pi a^4 \rho_b]$ is the Alfvén speed.

Thus, we can see that the magnetic power spectrum evolution is well approximated by $P(k, t) = P(k, t_i) e^{-k^2/k_D^2}$ for k values well separated from k_D . The evolution of the damping scale, k_D^{-1} , can be obtained by plugging this solution back in eq. (15). Doing so surprisingly yields the exact same equation as for compressible fluid, eq. (6).

While deriving the power spectrum evolution here and in the main Letter, we considered that $v_b \propto L_B$ on all scales. However, for $k > k_D$, the magnetic fields are being exponentially damped and for large enough k , the baryon flow should stop following the Lorentz force. However, as long as the scale where baryons stop following the Lorentz force is much smaller than k_D^{-1} we can safely assume $v_b \propto L_B$ to always be valid for the purpose of evaluating $P_B(k, t)$. In particular, one can see that L_B is roughly suppressed as $\sim k^2/k_D^2$ for $k > k_D$ while v_b can at best decrease with a dimensionless rate of $(H + \alpha)/H$. Consequently, v_b follows the Lorentz force until $k \gtrsim \sqrt{\alpha/H} k_D$. Prior to recombination, α is atleast 300 times larger than H , so baryons follow the Lorentz force deep into the damping regime.

Non-linear term in the baryon continuity equation

In this section we show that the non-linear term in the baryon continuity equation tends to enhance the baryon power spectrum when baryons are driven by magnetic fields.

We begin with the baryon continuity equation,

$$\frac{\partial \delta_b}{\partial t} + \frac{\nabla \cdot \vec{v}_b}{a} + \frac{\nabla \cdot (\vec{v}_b \delta_b)}{a} = 0. \quad (16)$$

Taking the Fourier transform of the above equation and then ensemble averaging with $\delta_b^*(k')$, we obtain

$$\left\langle \frac{\partial \delta_b(k)}{\partial t} \delta_b^*(k') \right\rangle + \frac{\langle \vec{k} \cdot \vec{v}_b(k) \delta_b^*(k') \rangle}{a} + \delta^3(k - k') \Xi(k) = 0, \quad (17)$$

where $\delta^3(k) = (2\pi)^3 \delta(k)$ and

$$\delta^3(k - k') \Xi(k) \equiv -\frac{i}{a} \int \frac{d^3 q}{(2\pi)^3} \langle (\vec{k} \cdot \vec{v}_b(q)) \delta_b(k - q) \delta_b^*(k') \rangle. \quad (18)$$

Here $\Xi(k)$ represents the contribution from the non-linear term in eq. (16) to the evolution of the baryon density power spectrum.

We are primarily interested in the regime where baryon perturbations become non-linear, i.e. where the Lorentz force dominates over the baryon thermal pressure and gravity. Consequently, v_b is determined by the balance between the Lorentz force and the photon drag force, $a\vec{v}_b \approx \vec{L}_B/(\alpha + H)$. Furthermore, assuming that δ_b is largely determined by the linear continuity equation, eq. (16), we have $\delta_b = -C\nabla \cdot v_b/[aH] = -C\nabla \cdot \vec{L}_B/[a^2 H(\alpha + H)]$, where C is some

constant of motion. As both v_b and δ_b are now expressed in terms of the Lorentz force, we can simplify eq. (18) to obtain Ξ in terms of the magnetic field power spectrum,

$$\Xi(k) = \frac{-4C^2[\delta_{ml}k_j - \delta_{mj}k_l](k_r k_s - k^2 \delta_{rs}/2)}{(4\pi a^4 \rho_b)^3 a^6 (H + \alpha)^3 H^2} \int d\Pi_q d\Pi_{q_1} [(k - q - q_1)_u (k - q - q_1)_v - (k - q - q_1)^2 \delta_{uv}/2] \\ \times (q_1 - q)_m M_{jr}(q_1) M_{lu}(q) M_{vs}(k - q_1), \quad (19)$$

where M is defined through $\langle B_i(k) B_j^*(k') \rangle \equiv \delta^3(k - k') M_{ij}(k')$ and $d\Pi_q = d^3q/(2\pi)^3$. While obtaining the above expression, we assumed the magnetic fields to be Gaussian distributed. In what follows, we shall show that Ξ is largely negative and hence leads to an enhancement of the baryon power spectrum.

We can further simplify the above integral by considering non-helical magnetic fields with M given by eq. (3) after setting $h(k) = 0$. Then after contracting over all indices and integrating over q , we obtain

$$\Xi(k) = \frac{C^2}{(4\pi a^4 \rho_b)^2 a^6 (H + \alpha)^3 H^2} \frac{1}{8} \frac{2V_A^2}{3} k^3 \int d\Pi_{q_1} P_B(q_1) \frac{P_B(k - q_1)}{(\vec{k} - \vec{q}_1)^2} \\ \left(k q_1 \left[q_1^3 (1 - 3x^2 + 2x^4) - k q_1^2 x (1 - 5x^2 + 4x^4) + k^2 q_1 (1 - 5x^2 + 4x^4) + k^3 x (1 - x^2) \right] \right. \\ \left. + k_{*2}^2 k_D^2 \left[2q_1^3 x^3 - 2k q_1^2 x^2 (x^2 + 2) + 3k^2 q_1 x (1 + x^2) - k^3 (1 + x^2) \right] \right). \quad (20)$$

where $x = (\vec{k} \cdot \vec{q}_1)/k q_1$, $V_A^2 = \int d\Pi_q P_B(q)/[4\pi a^4 \rho_b]$, and k_{*n} represents the moments of the magnetic power spectrum,

$$k_{*n}^n \equiv \frac{\int d\Pi_q q^n P_B(q)}{\int d\Pi_q P_B(q)}. \quad (21)$$

The integral in $\Xi(k)$ is similar to the integral in the power spectrum of the Lorentz force [63],

$$\langle \nabla \cdot \vec{L}_B(k) \nabla \cdot \vec{L}_B(k') \rangle = \delta^3(k - k') P_{\nabla \cdot \vec{L}_B} = \delta^3(k - k') \frac{k^4}{8(4\pi a^4 \rho_b)^2} \int \frac{d^3q}{(2\pi)^3} \frac{P_B(q) P_B(k - q)}{(k - q)^2} \left[k^2 (1 + x^2) - 4k q x^3 \right. \\ \left. + 2q^2 (1 - 2x^2 + 2x^4) \right]. \quad (22)$$

We have checked that our Lorentz force power spectrum matches to that used in literature [63].

Consequently, we rewrite Ξ in terms of $P_{\nabla \cdot \vec{L}_B}$ and use the fact that we have assumed $\delta_b = -C \nabla \cdot \vec{L}_B/[a^2 H(\alpha + H)]$, to obtain

$$\Xi(k) = \frac{C^2 P_{\nabla \cdot \vec{L}_B}}{a^6 (H + \alpha)^3 H^2} \frac{2k_D^2 V_A^2}{3} J(k, k_D) = \frac{2P_b(k)}{3} \frac{k_D^2 V_A^2}{a^2 (H + \alpha)} J(k, k_D), \quad (23)$$

where $\delta^3(k - k') P_b(k) = \langle \delta_b(k) \delta_b^*(k') \rangle$, and J is a dimensionless quantity that parametrizes the ratio of the integrals in Ξ and $P_{\nabla \cdot \vec{L}_B}$.

Since Ξ is proportional to P_b , we can effectively rewrite the continuity equation for baryon as

$$\frac{\partial \delta_b}{\partial t} + \frac{\nabla \cdot \vec{L}_B}{a(\alpha + H)} + \frac{2\delta_b}{3} \frac{k_D^2 V_A^2}{a^2 (H + \alpha)} J(k, k_D) = 0, \quad (24)$$

where we have used $a \vec{v}_b \approx \vec{L}_B/(\alpha + H)$. The above equation would yield the same equation for P_b as the original continuity equation when baryons are driven by the Lorentz force.

The above equation also allows us to confirm our original assumption of $\delta_b = -C \nabla \cdot \vec{L}_B/[a^2 H(\alpha + H)]$. To do so we simply substitute $\delta_b = -C \nabla \cdot \vec{L}_B/[a^2 H(\alpha + H)] \propto a^m$ in eq. (24) to obtain,

$$C = \frac{1}{m + \left[\frac{2}{3} \frac{k_D^2 V_A^2}{a^2 (H + \alpha)} J(k, k_D) \right]}. \quad (25)$$

Note that $\frac{k_D^2 V_A^2}{a^2 (H + \alpha)} \sim \mathcal{O}(1)$ according to the definition of k_D (eq. (6)). Consequently, the non-linear term in the continuity equation simply provides a correction of order J/m to the linear solution. In a radiation-dominated universe, we have $m = 3$ prior to the damping of the magnetic fields.

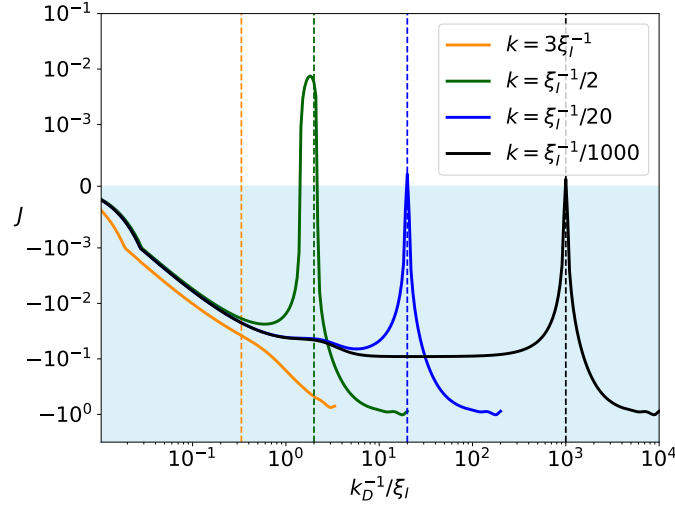


FIG. 4. Figure shows J , which is a dimensionless quantity that parametrizes the impact of the non-linear term in the baryon continuity equation, as a function of the damping scale, k_D^{-1} , for different values of k . The vertical dashed lines mark the points where $k_D = k$. We can see that J is almost always negative, except for small region near $k = k_D$. The negative values of J imply that the non-linear term enhances the linear baryon power spectrum.

In figure 4, we show J as a function of k_D for different values of k . Note that J is typically of order -0.1 for $k < k_D$. For $k \sim k_D$ we see J to jump to a small positive value and then it again becomes negative. The large negative values of J for $k \gg k_D$ have no physical significance because in that limit the magnetic fields and v_b are exponentially damped. Consequently, our calculation of Ξ , which is based on the assumption of $\delta_b \propto \vec{v}_b/a$, is no longer applicable. We instead expect Ξ to go to zero for $k \gg k_D$ because δ_b is no longer correlated with $\vec{v}_b \approx \vec{L}_B/(\alpha + H)$.

Hence, when the growth in δ_b is sourced by the magnetic fields, we expect the non-linear terms in the baryon continuity equation to provide a small enhancement to the baryon power spectrum obtained from linear analysis.